Tetrahedron: *Asymmetry* 21 (2010) 429–436

Contents lists available at ScienceDirect

Tetrahedron: *Asymmetry*

journal homepage: www.elsevier.com/locate/tetasy

Structurally constrained C_1-1,1′-bisisoquinoline-based chiral ligands: geometrical implications on enantioinduction in the addition of diethylzinc to aldehydes

Gao Qi, Zaher M. A. Judeh *

School of Chemical and Biomedical Engineering, Nanyang Technological University, 62 Nanyang Drive, N1.2 B1-14, Singapore 637459, Singapore

ARTICLE INFO

Article history:
Received 11 January 2010
Accepted 16 February 2010
Available online 8 April 2010

ABSTRACT

New highly constrained chiral C_1-1,1′-bisisoquinoline ligands have been synthesized. X-ray crystallographic analysis of these ligands showed peculiar structural differences between the parent 1′,2′,3′,4′-tetrahydro-1,1′-bisisoquinoline and its alkyl, acyl and sulfonyl derivatives. The consequences of their geometrical conformations on enantioinduction were examined by employing the enantioselective addition of diethylzinc to aldehydes. Such conformations greatly affected the catalytic efficiency of these ligands.

1. Introduction

Chiral *N*,*N*-ligands[1] have been used successfully in various asymmetric reactions.[2] However, the number and backbone variety of such diamines are rather limited, probably due to difficulties in their synthesis and resolution. The most well-studied and utilized chiral C_2-symmetric diamines include cyclohexane-1,2-diamine, 1,2-diphenylethan-1,2-diamine, 2,2′-diaminobinaphthyl and their derivatives.[3] On the other hand, C_2-symmetric 1,1′-bisisoquinolines (fully aromatic and partially reduced forms) such as **1–4** (Fig. 1) with their appealing backbone have recently been examined as new motifs for various asymmetric reactions.[4] Oxidative coupling of β-naphthol-2-carboxylate using **1** gave 1,1′-bis-β-naphthol-2-carboxylate in a maximum of 48% ee.[4a] Conjugate addition of diethylzinc to cyclohexenone using **2** gave ethylcyclohexanone in only 10% ee.[4b] Allylic alkylation of naphthyl substrates with EtMgBr using *N*-heterocyclic carbene **3** gave 35–73% ee.[4c] Allylation of benzaldehyde with allyl(trichloro)silane using *N*,*N*′-dioxide **4** gave 34–83% ee.[4d] A closer look at Figure 1 reveals that ligands **2–4** are C_2-symmetric structures and that the heterocyclic rings containing the chelating nitrogens are either fully saturated (**1** and **2**), partially saturated **3** or fully aromatic **4**. Such geometrical differences at the stereogenic centres have great effect on the enantioinduction.

Over the past few years, we have been interested in the chemistry of 1,1′-bisisoquinolines[5] and, in particular, their application as ligands for asymmetric catalysis. A careful study aimed at investigating the structural features responsible for their efficiency as chiral inducers is lacking. Therefore, we aimed to design and synthesize new C_1-1,1′-bisisoquinoline ligands (Fig. 2) with the intention of using them as probes to examine the effect of geometrical constrains on enantioinduction. The addition of Et_2Zn to aldehydes was considered as a model reaction. This reaction serves as a good testing ground for ligand development and optimization. It has attracted much attention because of its simplicity and utility for the preparation of chiral secondary alcohols which are key building blocks in the fine chemical and pharmaceutical industries.[6] Various chiral catalysts based on amino alcohols, diols, thiols, diselenides, disulfides, diamines, BINOLs, oxazaborolidines, bisoxazolidines and sulfinamides have been used successfully for the asymmetric addition of dialkylzincs to aldehydes.[6,7] The present ligand system is an aminopyridine type (Fig. 2) that has hardly been examined in this important transformation.[8] Therefore, it would also be very attractive to examine the use of this class of ligand in the asymmetric addition of Et_2Zn to various aldehydes.

Herein, we report on the design and synthesis of C_1-1,1′-bisisoquinolines **5a–e** (Fig. 2) and study the defining structural features responsible for their efficiency as chiral inducers with the aim of improving their performance and widening their scope in asymmetric catalysis. We also rationalize the yields and enantioselectivities of the products obtained from the additions of Et_2Zn to benzaldehyde based on the ligand's structural features deduced from the NMR spectroscopy and X-ray crystallographic analysis.

2. Results and discussion

Central to the present ligand's design is the idea of having heterocyclic ring **A** fully aromatic while ring **B** is fully saturated, consequently introducing C_1-symmetry to the framework. This design is anticipated to present diverse structural constraints compared to those observed in structures **1–4** (Fig. 1). The isoquinoline unit

* Corresponding author. Fax: +65 67947553.
E-mail address: zaher@ntu.edu.sg (Z.M.A. Judeh).

0957-4166/$ - see front matter © 2010 Elsevier Ltd. All rights reserved.
doi:10.1016/j.tetasy.2010.02.022

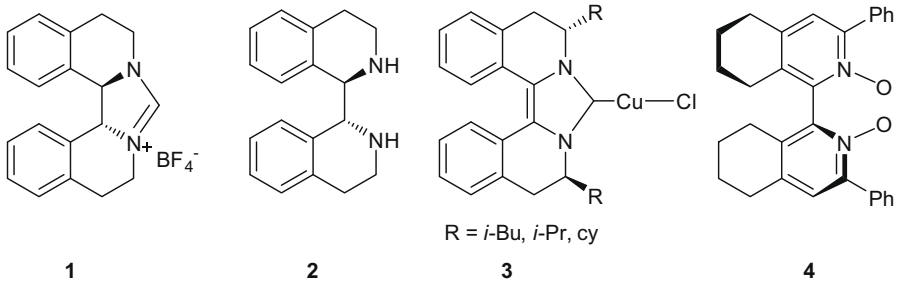

Figure 1. Chiral 1,1′-bisisoquinolines.

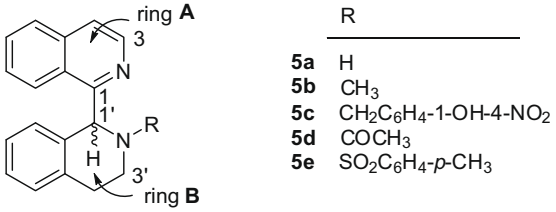

Figure 2. Chiral C_1-symmetric 1,1′-bisisoquinoline ligands **5a**–**e**.

with heterocyclic ring **A** is flat[9] due to its aromaticity while heterocyclic ring **B** is expected to have a twist-boat conformation.[5b,c] The bite angle between the two chelating nitrogens of ligands **5a**–**e** can be controlled by metal ions and substituents at the nitrogen of ring **B**. Compound *rac*-**5a** (Scheme 1) was synthesized under the double Bischler–Napieralski conditions.[10] Therefore, the treatment of bisoxamide **6** with polyphosphoric acid (PPA) at 190 °C furnished, unexpectedly, the C_1-symmetric compound *rac*-**5a** in 85% yield. Resolution of *rac*-**5a** was achieved using (*S*)-(+)-α-methyl benzyl isocyanate (Scheme 1).[10]

To introduce geometrical variations and examine the effects on enantioinduction, we carefully prepared chiral ligands (+)-**5b**–**e**. We rationalized that since there are no substituents at or next to the chelating nitrogens of (+)-**5a** (i.e., at both nitrogens or at carbons 3 and 3′), the active chiral space at the metal centre is relatively ill-defined especially when considering the free rotation around the C1–C1′ bond. We envisioned that the introduction of substituents of variable sizes at the nitrogen of ring **B** should lead to more rigid and well-defined chiral motifs. We expected that the greater rigidity afforded by (+)-**5b**–**e** would result in higher enantioinduction. Therefore we prepared *N*-methyl (+)-**5b**, nitrophenol (+)-**5c**, amide (+)-**5d** and sulfamide (+)-**5e** derivatives (Scheme 2) from (+)-**5a**. Reaction between (+)-**5a** and methyl iodide in the presence of K_2CO_3 in CH_3CN gave (+)-**5b** as a light yellow foam in 76% yield. Similarly, the reaction between (+)-**5a** and 2-hydroxy-4-nitro-benzyl bromide gave (+)-**5c** as an off-white foam in 91% yield. Treatment of (+)-**5a** with acetyl chloride in the presence of K_2CO_3 in THF proceeded to give (+)-**5d** as a white foam in 89% yield. Likewise, the reaction of (+)-**5a** with *p*-toluenesulfonyl chloride gave (+)-**5e** as a white foam in 99% yield (Scheme 2).

Next, ligand (+)-**5a** was used in the enantioselective addition of Et_2Zn to benzaldehyde **7a** to optimize the reaction conditions. Initially, the effect of amount of Et_2Zn was examined. Alcohol **8a** was obtained in 72% yield and 63% ee when a combination of 10 mol % of ligand (+)-**5a** and 2 mol equiv of Et_2Zn in dry THF/hexane (1/3, v/v) was employed (Table 1, entry 1). An increase in the amount of Et_2Zn from 2 (Table 1, entry 1) to 3 equiv (Table 1, entry 2) resulted in an increase in both the yield (to 95%) and the ee (to 73%) of alcohol **8a**. A further increase in the amount of Et_2Zn to 5 equiv resulted in an increase in the yield of **8a** to 97% and a decrease in its ee to 64% (Table 1, entry 3). Thus, the optimum amount of Et_2Zn is established to be 3 equiv. When THF was replaced by toluene or diethyl ether (Table 1, entries 4 and 5, respectively), **8a** was obtained in a lower ee of 59% and 65%, respectively, but in near quantitative 99% yields. An increase in the temperature from rt to 50 °C shortened the reaction time to just 3 h and gave **8a** in 99% yield and 62% ee (Table 1, entry 6). A decrease in the reaction temperature to 0 °C increased the ee to 80% and decreased the yield to 83% (Table 1, entry 7). A further decrease in the temperature to −40 °C

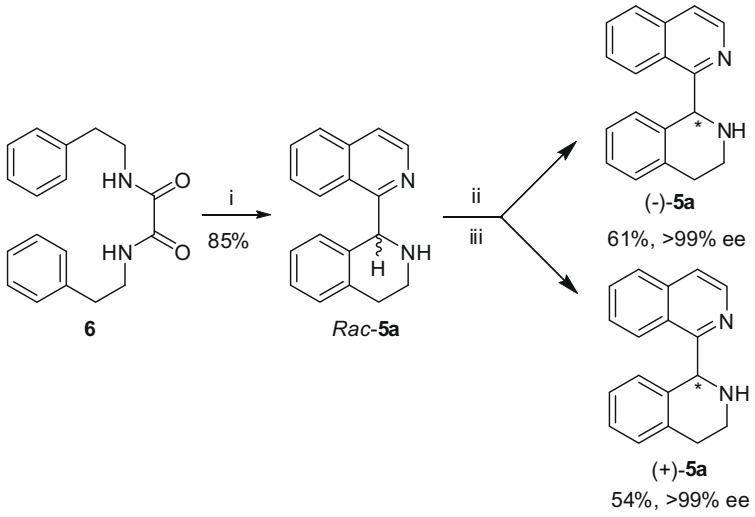

Scheme 1. Synthesis and resolution of ligand *rac*-**5a**. Reagents and conditions: (i) PPA, 190 °C, 18 h; (ii) (*S*)-(+)-α-methyl benzyl isocyanate, CH_2Cl_2, rt 30 min; (iii) NaOBu, *n*-BuOH, 110 °C, 3 h, recrystallization from EtOH.

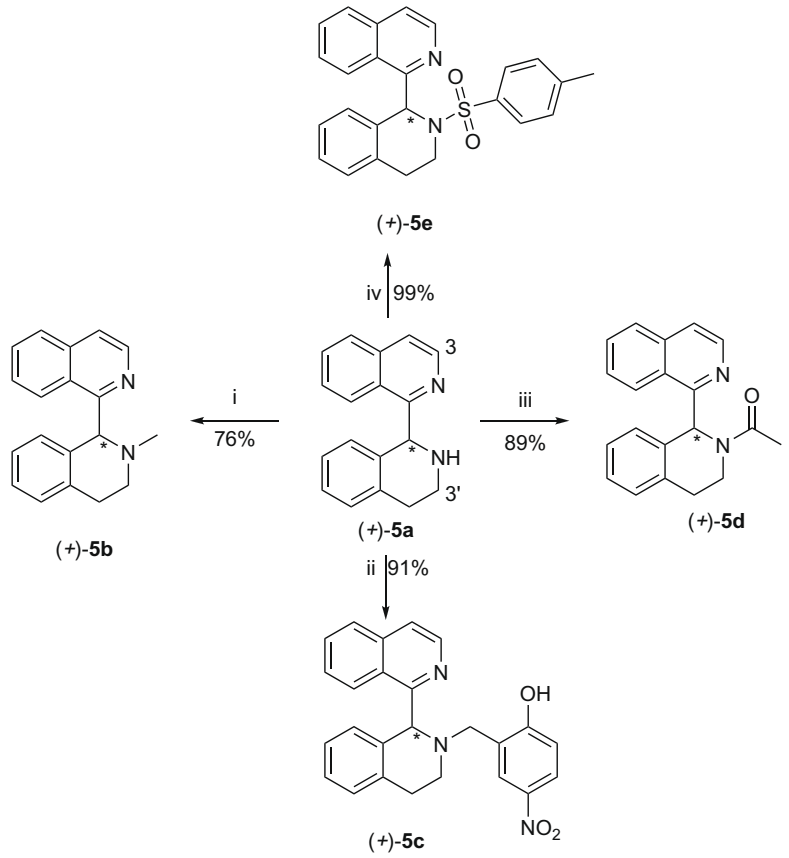

Scheme 2. Synthesis of ligands (+)-**5b**–**e**. Reagents and conditions: (i) 1.1 equiv CH_3I, K_2CO_3, CH_3CN, 50 °C, overnight; (ii) 1.1 equiv 2-hydro-5-nitro-benzylbromide, K_2CO_3, CH_3CN, 50 °C, overnight; (iii) 1.1 equiv, CH_3COCl, K_2CO_3, THF, 50 °C, overnight; (iv) 1.1 equiv TsCl, K_2CO_3, THF, 50 °C, overnight.

Table 1
Enantioselective addition of Et_2Zn to benzaldehyde **7a**

7a **8a**

Entry	Ligand (mol %)	Et_2Zn (equiv)	Solvent ratio (1:3; v/v)	Temp (°C)	Time (h)	Yield[a] (%)	ee[b] (%)
1	(+)-**5a** (10)	2	THF/hexane	rt	20	72	63
2	(+)-**5a** (10)	3	THF/hexane	rt	20	95	73
3	(+)-**5a** (10)	5	THF/hexane	rt	20	97	64
4	(+)-**5a** (10)	3	Toluene/hexane	rt	20	99	59
5	(+)-**5a** (10)	3	Et_2O/hexane	rt	20	99	65
6	(+)-**5a** (10)	3	THF/hexane	50	3	99	62
7	(+)-**5a** (10)	3	THF/hexane	0	30	83	80
8	(+)-**5a** (10)	3	THF/hexane	−40	40	9	26
9	(+)-**5a** (1)	3	THF/hexane	0	30	28	49
10	(+)-**5a** (5)	3	THF/hexane	0	30	62	72
11	(+)-**5a** (15)	3	THF/hexane	0	30	96	85
12	(+)-**5a** (20)	3	THF/hexane	0	30	57	82
13	(+)-**5a** (50)	3	THF/hexane	0	30	23	89
14	(+)-**5a** (100)	3	THF/hexane	0	30	9	90
15	(+)-**5b** (15)	3	THF/hexane	0	30	26	15 (*S*)
16	(+)-**5c** (15)	3	THF/hexane	0	30	22	0
17	(+)-**5d** (15)	3	THF/hexane	0	30	15	0
18	(+)-**5e** (15)	3	THF/hexane	0	30	13	0
19	—	3	THF/hexane	0	30	2	0

[a] Determined by GC using HP-5 column.
[b] Determined by GC using Chiraldex G-TA column. The (*R*)-configuration was determined by comparing the sign of specific rotation value with the literature value.[11a]

led to a dramatic decrease in both the yield (9%) and the ee (26%) of **8a** (Table 1, entry 8) presumably due to precipitation of the (+)-**5a**/Et_2Zn complex which can be clearly seen in the reaction tube. Further reactions were conducted at 0 °C to examine the optimum ligand loading. As seen in Table 1, entries 9–14, a general trend of increase in the ee (up to 90%) with increased loading of (+)-**5a** can be observed. Unfortunately, the increase in the ee was accompanied by a sharp fall in the yield of **8a** (Table 1, entries 11–14). The best result was obtained when a loading of 15 mol % of (+)-**5a** was used (Table 1, entry 11) whereby **8a** was obtained in 96% yield and 85% ee. Therefore, further reactions were conducted using these conditions.

Next, ligands **5b**–**e** were examined under the optimized conditions as shown in Table 1, entry 11. While addition of Et_2Zn to **7a** in the presence of (+)-**5b** gave **8a** in both low yield (26%) and ee (15%) (Table 1, entry 15), surprisingly, the addition of Et_2Zn in the presence of ligands (+)-**5c**, (+)-**5d** or (+)-**5e** gave **8a** again in low yields (22%, 15% and 13%, respectively) and startlingly in *racemic* form with no induction whatsoever (Table 1, entries 16–18). In the latter case, apparently, ligands (+)-**5c**–**e** were not involved in the catalytic cycle. To examine this view, the reaction was repeated under the same conditions but without ligands to examine the extent of reaction conversion (Table 1, entry 19). Here, **8a** was obtained in only 2% yield indicating the importance of the ligands in the catalytic cycle. Further to this, the addition of a solution of Et_2Zn to a sample of (+)-**5c** in $CDCl_3$ brought no significant chemical shift changes in the ^1H NMR spectrum in contrast to considerable shifts observed in the case of (+)-**5a**. More evidence for the non-involvement of ligands (+)-**5c**–**e** in the catalytic cycle was sought from the crystal structures of the ligands. Therefore, we attempted the crystallization of ligands **5a–e** to examine the structural arrangements and the extent of constrains in these ligands. All attempts to crystallize enantiopure compounds (+)-**5b**–**e** from various solvents were unsuccessful. Gratifyingly, crystallization of (−)-**5a**, *rac*-**5d** and *rac*-**5e** from ethanol gave single crystals suitable for X-ray anlysis.[12] Crystallographic analysis of (−)-**5a** revealed the following main features: (i) the C1–C1′ bridging bond between rings **A** and **B** is seen to be in the equatorial orientation with respect to the two heterocyclic rings. (ii) The

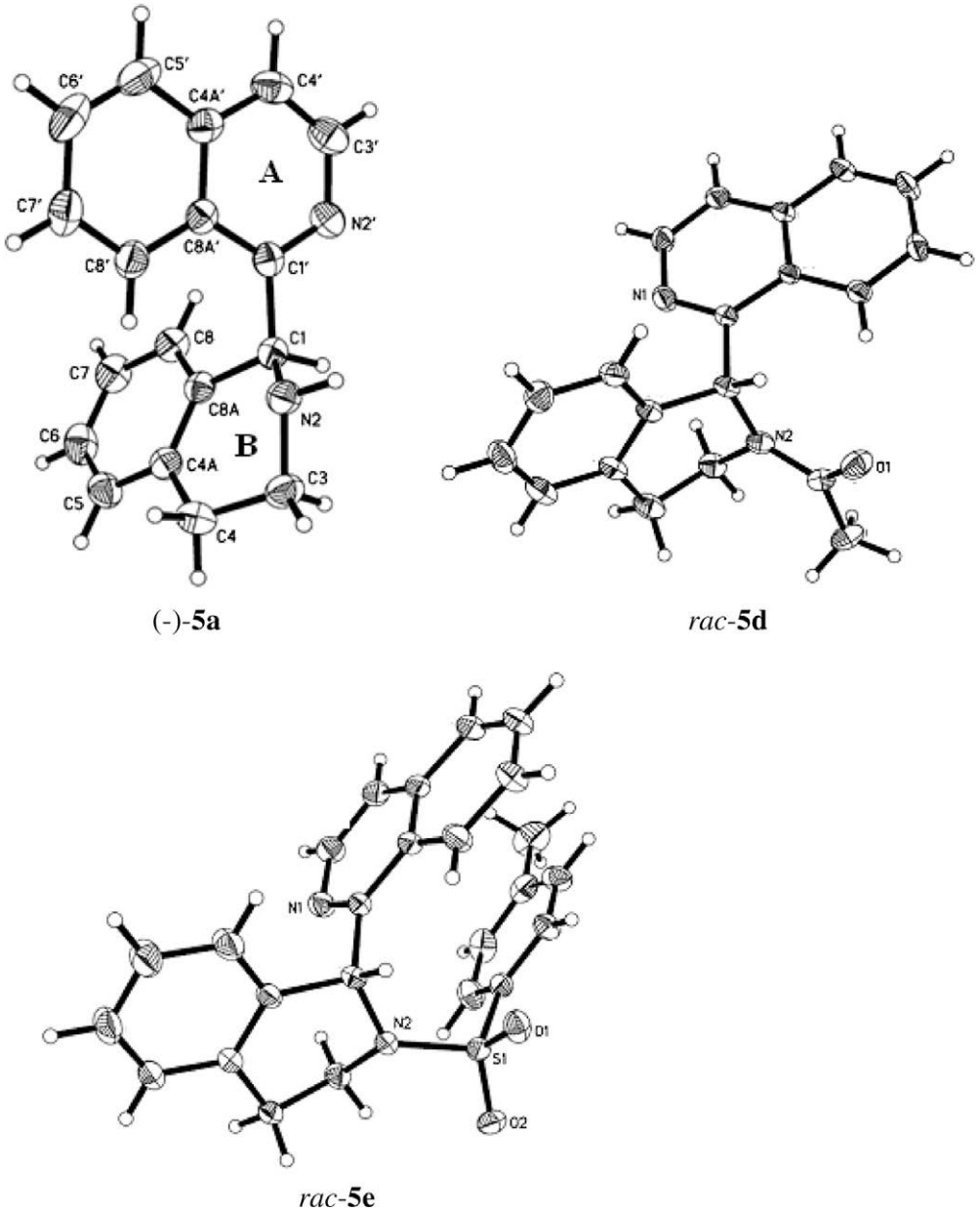

Figure 3. ORTEP diagram showing the crystal structures of (−)-**5a**, *rac*-**5d** and *rac*-**5e**.

two isoquinoline ring systems of (−)-**5a** are oriented with a small bias to the *syn* conformation with a C8a–C1–C1′–C8a′ dihedral angle of 62°. (iii) Heterocyclic ring **B** adopted a twist-boat conformation. (iv) The fully aromatic isoquinoline moiety (top portion of the structure) is projecting towards the main plane of ring **B**. These arrangements are in stark difference to the geometrical conformations observed in the C_2-symmetric structure **2** (Fig. 1) where the C1–C1′ bond is observed to be in the equatorial position and the two isoquinoline rings are in the *anti* orientation.[4b] This type of arrangement represents a fundamental geometrical preference observed in C_1- and C_2-1,1′-bisisoquinolines.

A closer look at the crystal structures of *rac*-**5d** and *rac*-**5e** (Fig. 3) reveals the following common features in both structures: (i) the C1–C1′ bridging bond between rings **A** and **B** is seen to be in the axial orientation with respect to the two heterocyclic rings; (ii) the fully aromatic isoquinoline moiety is projecting with an almost complete offset with respect to the main plane of the saturated ring **B** (lower portion of the structure); (iii) heterocyclic ring **B** adapted a twist-boat conformation. Comparing the crystal structures of (−)-**5a**, *rac*-**5d** and *rac*-**5e**, it can be seen that the two nitrogens in *rac*-**5d** and *rac*-**5e** are not sharing a common space and thus metal chelation to both of them is less likely. Moreover, the preferential conformations of *rac*-**5d** and *rac*-**5e** resulted in severe crowding at the chelating nitrogens and at the chiral core. Consequently, **8a** was formed in low yields and in racemic form. Such conformations are in stark contrast to that of (−)-**5a** where easy chelation is feasible. Although single X-ray quality crystals could not be obtained for ligands (+)-**5b** and (+)-**5c**, the structural arrangement of (+)-**5c** is expected to be similar to those of (+)-**5d** and (+)-**5e** which may explain the lack of enantioinduction observed. Moreover, the crowding at the chelating nitrogens of (+)-**5b** is expected to be less than that of (+)-**5c**, (+)-**5d** and (+)-**5e** since a methyl substituent is less bulky than a hydroxy nitrobenzyl, an acetyl or a tosyl group. This may explain the low enantioselectivity observed for (+)-**5b** (Table 1, entry 15). While we cannot rule out the contributions due to electronic effects on the enantioinduction, we strongly believe that the fundamental issue here is the lack of chelation of Et_2Zn to the nitrogens that mainly determines the course of selectivity due to the preferred conformations.

To study the scope and limitation of ligand (+)-**5a**, a number of aromatic aldehydes having electron-donating (**7b**–**h**) and electron-withdrawing (**7i**–**p**) substituents were examined along with **7q** and **7r** under the optimized conditions reported in Table 1, entry 11. In general, very good yields and enantioselectivities of the secondary alcohols **8a**–**r** were obtained (Table 2). The following observations can be made from Table 2: (i) electron-withdrawing substituents (Table 2, entries 9–16) gave better yields and enantioselectivities compared to poor (Table 2, entries 2–5) and strong (Table 2, entries 6–8) electron-donating substituents; (ii) generally, electron-donating substituents at the *ortho*-positions gave better enantioselectivities compared to the same substituents at the *para* and *meta* positions, while substituents at the *meta* positions gave better results compared to those at the *para* positions (see e.g., Table 2, entries 2–4 and entries 6–8); (iii) the substituent effect is more pronounced at the *ortho* position due to the steric bulkiness that these groups exert compared to the same *meta* or *para* substituents. In support of this fact, doubly substituted 2,6-dichlorobenzaldehyde gave the highest yield of 99% and highest ee of 87%; (iv) the

Table 2
Enantioselective addition of Et_2Zn to aldehydes catalyzed by (+)-**5a**

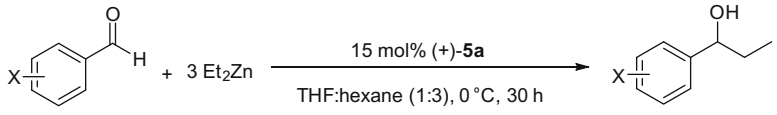

7a-r **8a-r**

Entry[a]	Aldehyde		Product	Yield[b] (%)	ee[c] (%)
1	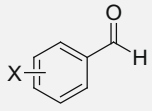	X = H **7a**	**8a**	96	85
2		X = *o*-CH_3 **7b**	**8b**	51	70
3		X = *m*-CH_3 **7c**	**8c**	69	65
4		X = *p*-CH_3 **7d**	**8d**	17	40
5		X = *p*-C_2H_5 **7e**	**8e**	38	71
6		X = *o*-MeO **7f**	**8f**	83	74
7		X = *m*-MeO **7g**	**8j**	82	73
8		X = *p*-MeO **7h**	**8h**	51	52
9		X = *o*-I **7i**	**8i**	95	73
10		X = *m*-I **7j**	**8j**	89	80
11		X = *p*-I **7k**	**8k**	59	66
12		X = *p*-F **7l**	**8l**	33	61
13		X = *p*-Cl **7m**	**8m**	90	72
14		X = *p*-Br **7n**	**8n**	52	71
15		X = 2,6-di-Cl **7o**	**8o**	99	87
16		X = *p*-F_3C **7p**	**8p**	88	72
17	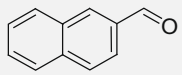	**7q**	**8q**	73[d]	81[e]
18	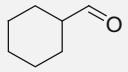	**7r**	**8r**	55	68

[a] Reaction conditions: 15 mol % (+)-**5a**, 3.0 equiv Et_2Zn, THF/hexane (1:3, v/v), 30 h, 0 °C.
[b] Determined by GC using Chiraldex G-TA column.
[c] Determined by GC using Chiraldex G-TA column. The configuration was determined by comparing the sign of specific rotation values with literature values.[11]
[d] Isolated yields.
[e] Determined by HPLC using a Chiral OD-H column.

ee increases with an increase in electronegativity of the *para*-halogens (except for entry 12, Table 2). Alkylation of β-naphthaldehyde **7q** and cyclohexanecarbaldehyde **7r** gave 81% and 68% ee, respectively (Table 2, entries 17 and 18, respectively).

3. Conclusion

New highly constrained chiral C_1-1,1′-bisisoquinoline ligands have been synthesized. Their geometrical conformations were found to greatly affect the catalytic efficiency and extensively influence the enantioinduction in the addition of Et_2Zn to benzaldehyde. X-ray crystallographic analysis of (−)-**5a**, *rac*-**5d** and *rac*-**5e** revealed peculiar structural features that were helpful in explaining the chelating and catalytic efficiencies of these ligands. The equatorial arrangement of the C1–C1′ bridging bond joining heterocyclic rings **A** and **B** of the C_1-1,1′-bisisoquinoline ligands seems to be essential for the high catalytic efficiency. Ligand (+)-**5a** afforded the desired secondary alcohols in excellent yield and up to 87% ee. Further studies using these ligands are currently under investigation in our laboratory.

4. Experimental

4.1. General

All commercial materials were used as received. Analytical thin layer chromatography (TLC) was performed using Merck 60 F_{254} precoated silica gel plate (0.2 mm thickness). Column chromatography was performed using Merck Silica Gel 60 (230–400 mesh). THF, diethyl ether and toluene were obtained from PURE SOLV PS-400-5-MD system. Melting points were determined on a Bamstead Electrothermal 9100 melting point tester. FTIR were recorded on a Perkin–Elmer FTIR system Spectrum BX. ^{1}H NMR spectra were recorded at 300 MHz and ^{13}C NMR spectra were recorded at 75.47 MHz on a Bruker Advanced DPX 300. Routine mass spectra were recorded on an ABI QSTAR Elite mass spectrometer. X-ray single crystal diffraction data were obtained on a Bruker-AXS Smart Apex CCD single-crystal diffractometer. HPLC was performed on an Agilent 1100 using Diacel chiralcel OD-H chiral column. GC was performed on an Agilent 6890 using Chiraldex G-TA, 30 m × 0.25 mm ID chiral column. Optical rotations were measured using a JASCO P-1020 polarimeter.

4.2. Preparation of (+)-*N*′-methyl-1′,2′,3′,4′-tetrahydro-1,1′-bisisoquinoline (+)-5b

Iodomethane (78.1 mg, 0.55 mmol) was added to a mixture of (+)-**5a** (130 mg, 0.5 mmol) and K_2CO_3 (138 mg, 1.0 mmol) in CH_3CN (4 mL). The mixture was heated overnight at 50 °C. The solvent was removed under vacuum and the solid formed was re-dissolved in a mixture of H_2O (10 mL) and CH_2Cl_2 (15 mL). The aqueous layer was separated and extracted further with CH_2Cl_2 (3 × 10 mL). The combined organic extracts were washed with brine, dried over $MgSO_4$, filtered and evaporated under vacuum till dryness. The off-white solid was purified by column chromatography (EtOAc) to give (+)-**5b** as light yellow foam (104.1 mg, 76%). Mp 89–93 °C. $[\alpha]_D^{25} = +159.7$ (*c* 1.13, CH_2Cl_2). FTIR (Nujol) ν_{max}: 2786, 1717, 1621, 1344, 1140, 822, 754, 736 cm^{-1}. ^{1}H NMR (300 MHz, $CDCl_3$) δ: 2.19 (3H, s, NC*H*$_3$), 2.74 (1H, m, *J* = 11.7 Hz, 3.6 Hz, 1 × H4′), 2.93 (1H, apparent d, *J* = 16.5 Hz, 1 × H4′), 3.25 (1H, ddd, *J* = 11.3 Hz, 5.7 Hz, 1.8 Hz, 1 × H3′), 3.50 (1H, ddd, *J* = 16.2 Hz, 11.7 Hz, 5.7 Hz, 1 × H3′), 4.98 (1H, s, H1′), 6.53 (1H, d, *J* = 7.8 Hz, Ar-H), 6.85 (1H, t, *J* = 7.5 Hz, Ar-H), 7.08 (1H, t, *J* = 7.4 Hz, Ar-H), 7.19 (1H, d, *J* = 7.5 Hz, Ar-H), 7.33 (1H, t, *J* = 7.2 Hz, Ar-H), 7.54 (1H, t, *J* = 7.5 Hz, Ar-H), 7.61 (1H, d, *J* = 5.7 Hz, Ar-H), 7.76 (1H, d, *J* = 8.1 Hz, Ar-H), 8.42 (1H, d, *J* = 8.7 Hz, Ar-H), 8.52 (1H, d, *J* = 5.7 Hz, Ar-H). ^{13}C NMR (75.6 MHz, $CDCl_3$) δ: 29.8 (C4′), 44.7 (N*C*H$_3$), 53.5 (C3′), 75.1 (C1′), 121.0, 125.9, 126.2, 126.4, 126.5, 126.9, 127.0, 127.3, 128.6, 129.7, 133.5, 137.3, 137.6, 141.1, 162.1 (15 × Ar-C). Mass (ESI) calcd for $C_{19}H_{18}N_2$: 274.15, found 275.13 (M+1).

4.3. Preparation of (+)-*N*′-(2-hydroxy-5-nitro-benzyl)-1′,2′,3′,4′-tetrahydro-1,1′-bisisoquinoline (+)-5c

2-Hydroxy-5-nitro-benzylbromide (58 mg, 0.28 mmol) was added to a mixture of (+)-**5a** (65 mg, 0.25 mmol) and K_2CO_3 (69 mg, 0.5 mmol) in CH_3CN (3 mL). The mixture was heated up to 50 °C and stirred overnight. The reaction mixture was cooled to room temperature, filtered and the solid was washed with CH_2Cl_2 (20 mL). The combined organic phases were evaporated under vacuum to dryness. The off-white solid residue was purified by column chromatography (EtOAc) to give (+)-**5c** as an off-white foam (93.5 mg, 91%). Mp 98–101 °C. $[\alpha]_D^{25} = +62.5$ (*c* 0.77, CH_2Cl_2). FTIR (Nujol) ν_{max}: 3058, 2832, 1588, 1491, 1337, 1288, 1091, 829, 750 cm^{-1}. ^{1}H NMR (300 MHz, $CDCl_3$) δ: 2.73–2.82 (1H, m, 1 × H4′), 2.92 (1H, d, *J* = Hz, 1 × H4′), 3.32–3.43 (2H, m, H3′), 3.52 (1H, d, *J* = 14.4 Hz, NC*H*H), 3.91 (1H, d, *J* = 14.1 Hz, NCH*H*), 5.60 (1H, s, H1′), 6.61 (1H, d, *J* = 7.8 Hz, Ar-H), 6.72 (1H, d, *J* = 9.0 Hz, Ar-H), 6.91 (1H, t, *J* = 7.5 Hz, Ar-H), 7.11 (1H, t, *J* = 7.4 Hz, Ar-H), 7.19 (1H, d, *J* = 6.9 Hz, Ar-H), 7.56–7.69 (3H, m, 3 × Ar-H), 7.83–7.86 (2H, m, 2 × Ar-H), 7.97 (1H, dd, *J* = 9.0 Hz, 2.7 Hz, Ar-H), 8.16 (1H, d, *J* = 8.4 Hz, Ar-H), 8.54 (1H, d, *J* = 5.7 Hz, Ar-H). ^{13}C NMR (75.6 MHz, $CDCl_3$) δ: 29.0 (C4′), 48.9 (C3′), 58.0 (N*C*H$_2$Ph), 69.0 (C1′), 116.5, 121.5, 122.1, 125.1, 125.2, 125.3, 126.5, 126.9, 127.2, 127.3, 127.91, 127.94, 129.0, 130.4, 133.5, 136.1, 137.3, 140.0, 142.0, 160.2, 163.7 (21 × Ar-C). Mass (ESI) calcd for $C_{25}H_{21}N_3O_3$: 411.16, found 412.07 (M+1).

4.4. Preparation of (+)-*N*′-ethanoyl-1′,2′,3′,4′-tetrahydro-1,1′-bisisoquinoline (+)-5d

Acetyl chloride (43.2 mg, 39.1 μl, 0.55 mmol) was added to a mixture of (+)-**5a** (130 mg, 0.5 mmol) and K_2CO_3 (138 mg, 1.0 mmol) in dry THF (5 mL) under a nitrogen atmosphere. The reaction mixture was stirred at 50 °C overnight. The solvent was removed under vacuum and the solid formed was re-dissolved in a mixture of H_2O (10 mL) and CH_2Cl_2 (15 mL). The aqueous layer was separated and extracted further with CH_2Cl_2 (3 × 10 mL). The combined organic extracts were washed with brine, dried over $MgSO_4$, filtered and evaporated till dryness under vacuum. The white solid residue was purified by column chromatography (EtOAc/hexane = 1/9) to give (+)-**5d** as **a** white foam (134.0 mg, 89%). Mp 97–99 °C. $[\alpha]_D^{25} = +399.4$ (*c* 0.65, CH_2Cl_2). FTIR (Nujol) ν_{max}: 3430, 1585, 1333, 1161, 1091, 971, 735, 667 cm^{-1}. ^{1}H NMR (300 MHz, $CDCl_3$) δ: 2.16 (3H, s, C*H*$_3$), 3.07–3.11 (2H, m, H4′), 3.81 (1H, m, *J* = 13.5 Hz, 3.9 Hz, 1 × H3′), 4.15–4.25 (1H, m, 1 × H3′), 6.88 (1H, d, *J* = 7.8 Hz, Ar-H), 7.07 (1H, m, *J* = 7.4 Hz, 1.5 Hz, Ar-H), 7.17 (1H, t, *J* = 7.2 Hz, Ar-H), 7.22 (1H, apparent d, *J* = 6.9 Hz, Ar-H), 7.53 (1H, d, *J* = 5.4 Hz, Ar-H), 7.67 (1H, s, H1′), 7.69–7.75 (2H, m, 2 × Ar-H), 7.80–7.83 (1H, m, Ar-H), 8.37 (1H, d, *J* = 5.4 Hz, Ar-H), 8.96 (1H, apparent d, *J* = 9.3 Hz, Ar-H). ^{13}C NMR (75.6 MHz, $CDCl_3$) δ: 21.8 (CO*C*H$_3$), 29.3 (C4′), 41.3 (C3′), 52.9 (C1′), 120.4, 126.0, 126.2, 126.7, 127.1, 127.3, 127.9, 128.0, 129.0, 130.1, 134.2, 136.1, 136.6, 141.7, 161.2 (15 × Ar-C), 169.2 (N*C*OCH$_3$). Mass (ESI) calcd for $C_{20}H_{18}N_2O$: 302.14, found 303.73 (M+1).

4.5. (+)-*N*′-Tosyl-1′,2′,3′,4′-tetrahydro-1,1′-bisisoquinoline (+)-5e

p-Toluene sulfonyl chloride (95 mg, 0.55 mmol) was added to a mixture of (+)-**5a** (130 mg, 0.5 mmol) and K_2CO_3 (138 mg,

1.0 mmol) in dry THF (5 mL) under a nitrogen atmosphere. The reaction mixture was stirred at 50 °C overnight. The reaction mixture was worked as described above to give white solid that was purified by column chromatography (EtOAc/hexane = 1/9) to give (+)-**5e** as white foam (204.5 mg, 99%). Mp 122–125 °C. $[\alpha]_D^{25} = +243.5$ (*c* 1.0, CH_2Cl_2). FTIR (Nujol) ν_{max}: 2912, 1643, 1430, 835, 769, 747, 635 cm^{-1}. ^1H NMR (300 MHz, $CDCl_3$) δ: 2.24 (3H, s, PhCH_3), 2.89–3.02 (2H, m, H4′), 3.91 (1H, m, *J* = 14.4 Hz, 4.4 Hz, 1 × H3′), 4.11–4.21 (1H, m, 1 × H3′), 6.81 (1H, d, *J* = 7.8 Hz, Ar-H), 6.88 (2H, apparent d, *J* = 7.8 Hz, 2 × Ar-H), 6.99 (1H, m, *J* = 6.9 Hz, 2.4 Hz, Ar-H), 7.07 (1H, s, H1′), 7.06–7.13 (2H, m, 2 × Ar-H), 7.28 (1H, apparent d, *J* = 8.1 Hz, 2Ar-H), 7.44 (1H, d, *J* = 5.4 Hz, Ar-H), 7.68–7.79 (3H, m, 3Ar-H), 8.21 (1H, d, *J* = 5.7 Hz, Ar-H), 8.80 (1H, apparent d, *J* = 9.3 Hz, Ar-H). ^{13}C NMR (75.6 MHz, $CDCl_3$) δ: 21.3 (PhCH_3), 27.8 (C4′), 40.5 (C3′), 55.7 (C1′), 120.3, 125.3, 126.1, 126.8, 126.9, 127.0, 127.17, 127.19, 128.0, 128.9, 129.2, 130.1, 133.8, 134.9, 136.6, 136.8, 141.8, 142.7, 160.1 (21 × Ar-C). Mass (ESI) calcd for $C_{25}H_{22}N_2O_2S$: 414.14, found 415.20 (M+1).

4.6. General procedure for the asymmetric addition of diethylzinc to aldehydes using (+)-5a

Ligand (+)-**5a** (39 mg, 0.15 mmol) was dissolved in THF (1 mL) and diethylzinc (3 mL, 1 M in hexane, 3 mmol) was added dropwise whereby an orange-red solution was obtained. The mixture was cooled down to 0 °C, stirred for 10 min. The aldehyde (1 mmol) was added via syringe and the reaction mixture was stirred at 0 °C for a specific time (TLC). The reaction was then quenched with saturated NH_4Cl (5 mL), washed with 1 N HCl (3 × 5 mL), saturated Na_2CO_3 (3 × 5 mL) and dried over $MgSO_4$ and filtered. The filtrate was subjected to GC directly or purified by column chromatography and then subjected to HPLC. The ee values were determined by GC using Chiraldex G-TA column or HPLC using Chiralcel OD-H column. The absolute configuration of the major enantiomer was assigned by making a comparison of the specific rotation value with literature values.

4.7. (1*R*)-1-Phenyl-1-propanol 8a (Table 2, entry 1)

The ee of 85% was determined by GC. GC (Chiraldex G-TA column) helium flow rate = 2.0 mL/min, oven = 110 °C, t_1 = 8.98 min for (*R*) and t_2 = 9.23 min for (*S*). $[\alpha]_D^{25} = +43.8$ (*c* 1.30, $CHCl_3$) {lit.[11a] $[\alpha]_D^{26} = +40.3$ (*c* 1.21, $CHCl_3$) for 96% ee (*R*)}.

4.8. (1*R*)-1-(2-Methylphenyl)-1-propanol 8b (Table 2, entry 2)

The ee of 70% was determined by GC. GC (Chiraldex G-TA column): helium flow rate = 2.0 mL/min, oven = 110 °C, t_1 = 16.44 min for (*R*) and t_2 = 18.82 min for (*S*). $[\alpha]_D^{25} = +40.5$ (*c* 0.45, $CHCl_3$) {lit.[11d] $[\alpha]_D^{18} = -43.0$ (*c* 0.97, CH_2Cl_2) for 78% ee (*S*)}.

4.9. (1*R*)-1-(3-Methylphenyl)-1-propanol 8c (Table 2, entry 3)

The ee of 65% was determined by GC. GC (Chiraldex G-TA column): helium flow rate = 2.0 mL/min, oven = 110 °C, t_1 = 14.18 min for (*R*) and t_2 = 14.56 min for (*S*). $[\alpha]_D^{25} = +38.7$ (c = 0.68, $CHCl_3$) {lit.[11b] $[\alpha]_D^{25} = +37.9$ (*c* 1.76, $CHCl_3$) for 95% ee (*R*)}.

4.10. (1*R*)-1-(4-Methylphenyl)-1-propanol 8d (Table 2, entry 4)

The ee of 40% was determined by GC. GC (Chiraldex G-TA column): helium flow rate = 2.0 mL/min, oven = 110 °C, t_1 = 13.37 min for (*R*) and t_2 = 13.63 min for (*S*). $[\alpha]_D^{25} = +18.3$ (c = 0.21, $CHCl_3$) {lit.[11d] $[\alpha]_D^{18} = -27.7$ (*c* 1.24, CH_2Cl_2) for 65% ee (*S*)}.

4.11. (+)-1-(4-Ethylphenyl)-1-propanol 8e (Table 2, entry 5)

The ee of 71% was determined by GC. GC (Chiraldex G-TA column): helium flow rate = 3.0 mL/min, oven = 130 °C, t_1 = 6.50 min for (+) and t_2 = 6.57 min for (−). $[\alpha]_D^{25} = +21.3$ (*c* 1.22, $CHCl_3$).

4.12. (1*R*)-1-(2-Methoxyphenyl)-1-propanol 8f (Table 2, entry 6)

The ee of 74% was determined by GC. GC (Chiraldex G-TA column): helium flow rate = 2.0 mL/min, oven = 110 °C, t_1 = 31.22 min for (*R*) and t_2 = 33.57 min for (*S*). $[\alpha]_D^{25} = +19.6$ (*c* 0.85, $CHCl_3$) {lit.[11a] $[\alpha]_D^{26} = +23.7$ (*c* 1.40, $CHCl_3$) for 95% ee (*R*)}.

4.13. (1*R*)-1-(3-Methoxyphenyl)-1-propanol 8g (Table 2, entry 7)

The ee of 73% was determined by GC. GC (Chiraldex G-TA column): helium flow rate = 2.0 mL/min, oven = 110 °C, t_1 = 42.94 min for (*R*) and t_2 = 45.08 min for (*S*). $[\alpha]_D^{25} = +22.8$ (*c* 0.43, $CHCl_3$) {lit.[11a] $[\alpha]_D^{26} = +40.3$ (*c* 1.21, $CHCl_3$) for 95% ee (*R*)}.

4.14. (1*R*)-1-(4-Methoxyphenyl)-1-propanol 8h (Table 2, entry 8)

The ee of 52% was determined by GC. GC (Chiraldex G-TA column): helium flow rate = 2.0 mL/min, oven = 110 °C, t_1 = 39.71 min for (*R*) and t_2 = 40.98 min for (*S*). $[\alpha]_D^{25} = +20.3$ (*c* 0.76, $CHCl_3$) {lit.[11a] $[\alpha]_D^{26} = +38.9$ (*c* 1.23, $CHCl_3$) for 96% ee (*R*)}.

4.15. (+)-1-(2-Iodophenyl)-1-propanol 8i (Table 2, entry 9)

The ee of 73% was determined by GC. GC (Chiraldex G-TA column): helium flow rate = 3.0 mL/min, oven = 130 °C, t_1 = 21.10 min for (−) and t_2 = 24.12 min for (+). $[\alpha]_D^{25} = +17.8$ (*c* 1.71, $CHCl_3$).

4.16. (+)-1-(3-Iodophenyl)-1-propanol 8j (Table 2, entry 10)

The ee of 80% was determined by GC. GC (Chiraldex G-TA column): helium flow rate = 3.0 mL/min, oven = 130 °C, t_1 = 27.27 min for (+) and t_2 = 29.26 min for (−). $[\alpha]_D^{25} = +15.3$ (*c* 1.70, $CHCl_3$).

4.17. (+)-1-(4-Iodophenyl)-1-propanol 8k (Table 2, entry 11)

The ee of 66% was determined by GC. GC (Chiraldex G-TA column): helium flow rate = 3.0 mL/min, oven = 130 °C, t_1 = 28.16 min for (+) and t_2 = 29.45 min for (−). $[\alpha]_D^{25} = +16.8$ (*c* 0.85, $CHCl_3$).

4.18. (1*R*)-1-(4-Fluorophenyl)-1-propanol 8l (Table 2, entry 12)

The ee of 61% was determined by GC. GC (Chiraldex G-TA column): helium flow rate = 3.0 mL/min, oven = 130 °C, t_1 = 3.50 min for (*R*) and t_2 = 3.64 min for (*S*). $[\alpha]_D^{25} = +23.5$ (*c* 0.30, $CHCl_3$) {lit.[11e] $[\alpha]_D = +29.7$ (*c* 3.0, $CHCl_3$) for 79% ee (*R*)}.

4.19. (1*R*)-1-(4-Chlorophenyl)-1-propanol 8m (Table 2, entry 13)

The ee of 72% was determined by GC. GC (Chiraldex G-TA column): helium flow rate = 3.0 mL/min, oven = 130 °C, t_1 = 9.19 min for (*R*) and t_2 = 9.58 min for (*S*). $[\alpha]_D^{25} = +21.7$ (*c* 2.31, $CHCl_3$) {lit.[11a] $[\alpha]_D^{26} = +30.6$ (*c* 2.08, $CHCl_3$) for 96% ee (*R*)}.

4.20. (1*R*)-1-(4-Bromophenyl)-1-propanol 8n (Table 2, entry 14)

The ee of 71% was determined by GC. GC (Chiraldex G-TA column): helium flow rate = 3.0 mL/min, oven = 130 °C,

t_1 = 15.14 min for (*R*) and t_2 = 15.88 min for (*S*). $[\alpha]_D^{25} = +23.4$ (*c* 0.61, $CHCl_3$) {lit.[11c] $[\alpha]_D^{20} = +26.7$ (*c* 1.50, $CHCl_3$) for 98% ee (*R*)}.

4.21. (−)-1-(2,6-Dichlorophenyl)-1-propanol 8o (Table 2, entry 15)

The ee of 87% was determined by GC. GC (Chiraldex G-TA column): helium flow rate = 3.0 mL/min, oven = 130 °C, t_1 = 13.29 min for (+) and t_2 = 13.74 min for (−). $[\alpha]_D^{25} = -16.4$ (*c* 1.82, $CHCl_3$).

4.22. (*1R*)-1-(4-Trifluoromethylphenyl)-1-propanol 8p(Table 2, entry 16)

The ee of 72% was determined by GC. GC (Chiraldex G-TA column): helium flow rate = 2.0 mL/min, oven = 110 °C, t_1 = 12.34 min for (*R*) and t_2 = 13.18 min for (*S*). $[\alpha]_D^{25} = +15.8$ (*c* 1.30, $CHCl_3$) {lit.[11c] $[\alpha]_D^{20} = +18.6$ (*c* 3.40, $CHCl_3$) for 98% ee (*R*)}.

4.23. (*1R*)-1-(2-Naphthyl)-1-propanol 8q (Table 2, entry 17)

The ee of 81% was determined by HPLC. HPLC (Chiralcel OD-H column): hexane/IPA = 95/5, 1.0 mL/min, 25 °C, 254 nm, t_1 = 14.93 min for (*S*) and t_2 = 17.09 min for (*R*). $[\alpha]_D^{25} = +28.6$ (*c* 0.77, $CHCl_3$) {lit.[11c] $[\alpha]_D^{20} = +35.1$ (*c* 2.40, $CHCl_3$) for 92% ee (*R*)}.

4.24. (*1R*)-1-Cyclohexylpropanol 8r (Table 2, entry 18)

The ee of 68% was determined by GC. GC (Chiraldex G-TA column): helium flow rate = 1.0 mL/min, oven = Gradient 65–95 °C, t_1 = 52.50 min for (*R*) and t_2 = 53.33 min for (*S*). $[\alpha]_D^{25} = +6.6$ (*c* 0.65, $CHCl_3$) {lit.[11a] $[\alpha]_D^{26} = +5.4$ (*c* 0.61, $CHCl_3$) for 93% ee (*R*)}.

Acknowledgement

We gratefully acknowledge the Nanyang Technological University for financial support (Grant No. RG27/07).

References

1. Jean-Claude, K. *Chem. Rev.* **2008**, *108*, 140–205.
2. (a) Martins, J. E. D.; Morris, D. J.; Wills, M. *Tetrahedron Lett.* **2009**, *50*, 688–692; (b) Bandini, M.; Melucci, M.; Piccinelli, F.; Sinisi, R.; Tommasi, S.; Umani-Ronchi, A. *Chem. Commun.* **2007**, *43*, 4519–4521; (c) Wang, S.; Seto, C. T. *Org. Lett.* **2006**, *8*, 3979–3982; (d) Kina, A.; Ueyama, K.; Hayashi, T. *Org. Lett.* **2005**, *7*, 5889–5892; (e) Alexakis, A.; Tomassini, A.; Andrey, O.; Bernardinelli, G. *Eur. J. Org. Chem.* **2005**, *7*, 1332–1339.
3. (a) Bennani, Y. L.; Hanessian, S. *Chem. Rev.* **1997**, *97*, 3161–3195; (b) Anaya de Parrodi, C.; Juaristi, E. *Synlett* **2006**, 2699–2715; (c) Achard, T. R. J.; Clutterbuck, L. A.; North, M. *Synlett* **2005**, 1828–1847; (d) Ooi, T.; Ohmatsu, K.; Uraguchi, D.; Maruoka, K. *Tetrahedron Lett.* **2004**, *45*, 4481–4484; (e) Bayardon, J.; Sinou, D. *Synthesis* **2005**, *3*, 425–428.
4. (a) Arai, S.; Takita, S.; Nishida, A. *Eur. J. Org. Chem.* **2005**, 5262–5267; (b) Cavell, K. J.; Elliott, M. C.; Nielsen, D. J.; Paine, J. S. *Dalton Trans.* **2006**, 4922–4925; (c) Seo, H.; Hirsch-Weil, D.; Abboud, K. A.; Hong, S. *J. Org. Chem.* **2008**, *73*, 1983–1986; (d) Hrdina, R.; Dračínskỳ, M.; Valterová, I.; Hodačová, J.; Císaová, I.; Kotora, M. *Adv. Synth. Catal.* **2008**, *350*, 1449–1456.
5. (a) Shen, H. Y.; Ying, L. Y.; Jiang, H. L.; Judeh, Z. M. A. *Int. J. Mol. Sci.* **2007**, *8*, 505–512; (b) Craig, D. C.; Judeh, Z. M. A.; Read, R. *Tetrahedron* **2003**, *59*, 461–472; (c) Busato, S.; Craig, D. C.; Judeh, Z. M. A.; Read, R. *Aust. J. Chem.* **2002**, *55*, 733–736; (d) Judeh, Z. M. A.; Ching, C. B.; Bu, J.; McCluskey, A. *Tetrahedron Lett.* **2002**, *43*, 5089–5091.
6. (a) Noyori, R. *Asymmetric Catalysis in Organic Synthesis*; Wiley: New York, 1994; (b) Soai, K.; Shibata, T.. In *Comprehensive Asymmetric Catalysis*; Jacobsen, E. N., Pfaltz, A., Yamamoto, H., Eds.; Springer: Berlin, Germany, 1999; Vol. 2, pp 911–922.
7. For comprehensive reviews, see: (a) Pu, L.; Yu, H.-B. *Chem. Rev.* **2001**, *101*, 757–824; (b) Soai, K.; Niwa, S. *Chem. Rev.* **1992**, *92*, 833–856; (c) Noyori, R.; Kitamura, M. *Angew. Chem., Int. Ed.* **1991**, *30*, 49–69; Other literature see: (d) Mori, M.; Nakai, T. *Tetrahedron Lett.* **1997**, *38*, 6233–6236; (e) Zhang, F. Y.; Yip, C. W.; Cao, R.; Chan, A. S. C. *Tetrahedron: Asymmetry* **1997**, *8*, 585–589; (f) Shen, X.; Guo, H.; Ding, K. L. *Tetrahedron: Asymmetry* **2000**, *11*, 4321–4327; (g) Zhang, F. Y.; Chan, A. S. C. *Tetrahedron: Asymmetry* **1997**, *8*, 3651–3655; (h) Huang, Z.; Lai, H.; Qin, Y. *J. Org. Chem.* **2007**, *72*, 1373–1378; (i) Xiao, F. Y.; Takuji, H.; Guang, Y. Z. *Tetrahedron: Asymmetry* **2008**, *19*, 1670–1675; (j) José, E. D.; Martins, M. W. *Tetrahedron: Asymmetry* **2008**, *19*, 1250–1255; (k) Jiang, F. Y.; Liu, B.; Dong, Z. B.; Li, J. S. *J. Organomet. Chem.* **2007**, *692*, 4377–4380; (l) Manabu, H.; Takashi, M.; Kazuaki, I. *J. Org. Chem.* **2006**, *71*, 6474–6484; (m) Tanaka, T.; Yasuda, Y.; Hayashi, M. *J. Org. Chem.* **2006**, *71*, 7091–7093; (n) Liu, S.; Wolf, C. *Org. Lett.* **2007**, *9*, 2965–2968; (o) Blay, G.; Fernández, I.; Olmos, V. H.; Marco-Aleixandre, A. G.; Pedro, J. R. *J. Mol. Catal. A: Chem.* **2007**, *276*, 235–243; (p) Shi, M.; Sui, W. S. *Tetrahedron: Asymmetry* **1999**, *10*, 3319–3325; (q) Burguete, M. I.; Collado, M.; Escorihuela, J.; Luis, S. V. *Angew. Chem., Int. Ed.* **2007**, *46*, 9002–9005; (r) Schmidt, B.; Seebach, D. *Angew. Chem., Int. Ed.* **1991**, *30*, 1321–1323; (s) Shaohua, G.; Judeh, Z. M. A. *Tetrahedron Lett.* **2009**, *50*, 281–283; (t) Tanaka, T.; Sano, Y.; Hayashi, M. *Chem. Asian J.* **2008**, *3*, 1465–1471.
8. Cheng, Y. Q.; Bian, Z.; Kang, C. Q.; Guo, H. Q.; Gao, L. X. *Tetrahedron: Asymmetry* **2008**, *19*, 1572–1575.
9. Xi, H. W.; Judeh, Z. M. A.; Lim, K. H. *J. Mol. Struct.: Theochem.* **2009**, *897*, 22–32.
10. Gao, Q.; Judeh, Z. M. A. *Tetrahedron*, in press.
11. (a) Zhang, J. C.; Guo, H. C.; Wang, M. G.; Yin, M. M.; Wang, M. *Tetrahedron: Asymmetry* **2007**, *18*, 734–741; (b) Bisai, A.; Singh, P. K.; Singh, V. K. *Tetrahedron.* **2007**, *63*, 598–601; (c) Bulut, A.; Aslan, A.; Izgü, E. C.; Dogan, O. *Tetrahedron: Asymmetry* **2007**, *18*, 1013–1016; (d) Lin, R. X.; Chen, C. P. *J. Mol. Catal. A: Chem.* **2006**, 89–98; (e) Vyskočil, Š.; Jaracz, S.; Smrčina, M.; Kočovsky, P. *J. Org. Chem.* **1998**, *63*, 7727–7737.
12. *X-ray crystallographic data for* (−)-**5a**: Formula $C_{18}H_{16}N_2$, M = 260, orthorhombic, space group $P2(1)2(1)2(1)$, a = 6.9631(3) Å, b = 8.6098(4) Å, c = 22.6379(10) Å, β = 90°, V = 1357.16(10) Å^3, D_{calcd} = 1.274 Mg/m^3, Z = 4. 1.80° < θ < 26.45°. The number of reflections was 1630 considered to be observed of 9107 unique data. Final R indices ($I > 2\sigma(I)$) R_1 = 0.0303, wR_2 = 0.0943. Compound *rac*-**5d**: Formula $C_{20}H_{18}N_2O$, M = 302, triclinic, space group $P\bar{1}$, a = 7.4307(4) Å, b = 10.0093(4) Å, c = 11.5391(6) Å, β = 89.319(3)°, V = 771.31(7) Å^3, Z = 2, D_{calcd} = 1.302 Mg/m^3, 1.92° < θ < 30.00°. The number of reflections was 4487 considered to be observed of 20076 unique data. Final R indices ($I > 2\sigma(I)$) R_1 = 0.1096, wR_2 = 0.2686. Compound *rac*-**5e**: Formula $C_{25}H_{22}N_2O_2S$, M = 414, triclinic, space group $P\bar{1}$, a = 8.1599(3) Å, b = 9.1169(3) Å, c = 14.7016(4) Å, β = 83.359(2)°. V = 1000.55(6) Å^3, Z = 2, D_{calcd} = 1.376 Mg/m^3, 1.40° < θ < 32.88°. The number of reflections was 7416 considered to be observed of 28209 unique data. Final R indices ($I > 2\sigma(I)$) R_1 = 0.0537, wR_2 = 0.1615. CCDC 746424, 746425 and 746426 contain the supplementary crystallographic data for this paper. These data can be obtained free of charge from The Cambridge Crystallographic Data Centre via http://www.ccdc.cam.ac.uk/data_request/cif.